Update on FDC Algorithm Development

Simon Taylor and Daniel S. Carman
Ohio University

March 9, 2006

Abstract

We report progress in obtaining charge and timing information from the Struck Flash ADC. We also present results for an improved method for obtaining the centroid of the charge distributed over several strips.

This document provides an update on studies of the FDC prototype geared toward improving algorithms for extracting charge, centroids, and timing from the strip data. In order to save money, we are considering instrumenting both the anode wires and the cathode strips with flash-ADCs. If that is the case, we need to be able to extract both the time of the event and the charge from the flash-ADC data. Most of the article describes progress toward using the first few samples in leading edge of the digitized pulse to find the time of the event. The last section describes an improved method for finding the centroid of the charge distributed over three adjacent strips.

1 Charge Extraction

The extraction of the charge is in principle straight-forward: one integrates the ADC counts above the background for each strip and wire in the system. Instead of using a simple unweighted sum of the samples above the background, we use the so-called "Extended Simpson's rule"[1]:

$$\int_{t_1}^{t_N} f(t)dt = \Delta t \left[\frac{1}{3}f_1 + \frac{4}{3}f_2 + \frac{2}{3}f_3 + \frac{4}{3}f_4 + \cdots + \frac{2}{3}f_{N-2} + \frac{4}{3}f_{N-1} + \frac{1}{3}f_N\right] + \mathcal{O}\left(\frac{1}{N^4}\right), \quad (1)$$

where Δt is the step size and $f_i = f(t_i)$ is value of the function at t_i approximated by the data. For the lower limit of the integration we look for leading edge that exceeds some threshold T in statistically significant way:

$$f_2 - f_1 > \sqrt{\delta f_2^2 + \delta f_1^2}, \quad f_2 > T. \tag{2}$$

For the upper limit of the integration we require two successive samples to be consistent with zero:

$$f_{N-1} < \delta f_{N-1}, \quad f_N < \delta f_N. \tag{3}$$

For the studies below the threshold was set to 5 mV. Figure 1 demonstrates that a simple unweighted sum of the samples overestimates the integral relative to the Extended Simpson's rule result by a small amount; in our case this amounts to about 0.36% on average, with the spread in the difference between the two methods becoming large for small pulse heights.

2 Timing methods

The simplest method for extracting the time is to record the time bin at which the data exceeds the threshold T. The timing resolution of this method is limited by the bin size; namely, $\sigma_t = \Delta t/\sqrt{12}$ (= 2.75 ns for the 105 MS/s Struck FADC we are using). In order to do better than this we need to use more samples in the rising edge of the pulse in conjunction with a suitable model for the shape of the pulse.

The current induced on the anode wire due to an avalanche is given by

$$i(t) = \begin{cases} -q_a \frac{C}{4\pi\varepsilon_0} \frac{1}{t+t_0} & \text{for } t \geq 0 \\ 0 & \text{for } t < 0 \end{cases} \tag{4}$$

where

$$t_0 = \frac{\pi a^2 \varepsilon_0}{\mu C V_0}, \tag{5}$$

for which q_a is the anode charge, a is the radius of the anode wire, C is the capacitance per unit length for the system, $\varepsilon_0 \approx 8.85$ pF/m is the permittivity of the gas, μ is the mobility of the positive ions in the gas, and V_0 is the voltage on the anode wires. For our prototype configuration $t_0 \approx 1.1$ ns. The image of the anode charge is seen on both cathode planes distributed over several

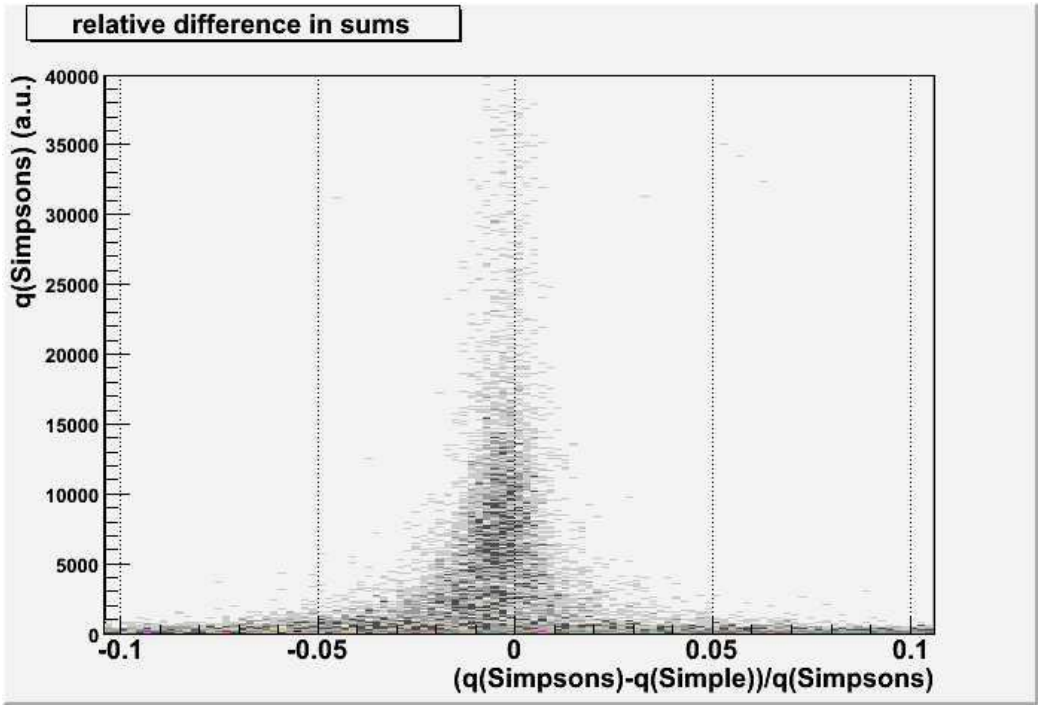

Figure 1: Relative difference between two methods for calculating the charge from the FADC data as a function of the charge.

strips. The signals induced on the strips have the same time dependence as the signal on the wire; *i.e*,

$$i_c(\lambda, t) = \frac{q_c(\lambda)}{t + t_0} \text{ for } t \geq 0, \tag{6}$$

where $q(\lambda)$ is the induced charge at $\lambda = x/h$ in the strip coordinate x relative to the anode-cathode separation h.

The preamplifier/postamplifier electronics modifies this time behavior. For simplicity we assume that the transfer function for the pre-amplifier/post-amplifier chain has a single pole. In the frequency domain,

$$H(s) = \frac{-R_F}{1 + s\tau}, \tag{7}$$

which translates to an exponential distribution in the time domain:

$$h(t) = \frac{-R_F}{\tau} e^{-t/\tau}. \tag{8}$$

The measured voltage as a function of time is a convolution of $i(t)$ with $h(t)$:

$$V(t) = \int_0^t i(t')h(t - t')dt'. \tag{9}$$

The result of this integration is

$$V(\lambda, t) = -\frac{q_c(\lambda)R_F}{\tau} e^{-(t+t_0)/\tau} \left[Ei\left(\frac{t + t_0}{\tau}\right) - Ei\left(\frac{t_0}{\tau}\right) \right] \text{ for } t \geq 0. \tag{10}$$

where $Ei(x)$ is the "exponential integral":

$$Ei(x) \equiv \int_{-\infty}^{x} \frac{e^z}{z} dz. \tag{11}$$

The Taylor series expansion for $Ei(x)$ is

$$Ei(x) = \gamma + \ln x + \frac{x}{1 \cdot 1!} + \frac{x^2}{2 \cdot 2!} + \cdots + \frac{x^n}{n \cdot n!} + \cdots, \tag{12}$$

where $\gamma = 0.577256649...$ is Euler's constant. For large x, the asymptotic expression is

$$Ei(x) \sim \frac{e^x}{x} \left(1 + \frac{1!}{x} + \frac{2!}{x^2} + \cdots + \frac{n!}{x^n} + \cdots\right). \tag{13}$$

After translating in time (and assuming the background in the real signal has been subtracted),

$$V(\lambda,t)=\begin{cases} -\frac{q_c(\lambda)R_F}{\tau}e^{-(t-t_{min}+t_0)/\tau}\left[Ei\left(\frac{t-t_{min}+t_0}{\tau}\right)-Ei\left(\frac{t_0}{\tau}\right)\right] & \text{for } t\geq t_{min}, \\ 0 & \text{for } t<t_{min} \end{cases} \tag{14}$$

To find t_{min} and q_c we used a modification of the Newton-Raphson method[2]. We used the first four samples (starting at the sample one time bin before the one that exceeds the threshold T) in the rising edge of the pulse. This leads to a system of four equations in two unknowns:

$$F_i = V_i - |V(\lambda,t_i;t_{min},q_c)| = 0, \tag{15}$$

where V_i is the sampled pulse height at time t_i.

The Newton-Raphson method is an iterative procedure based on a Taylor expansion of F_i, assuming that $\vec{x}=\{q_c,t_{min}\}$ is sufficiently close to the right set of roots for $\vec{F}$:

$$F_i(\vec{x}+\delta\vec{x}) = F_i(\vec{x}) + \sum_j \frac{\partial F_i}{\partial x_j}\delta x_j + \mathcal{O}(\delta\vec{x}^2), \tag{16}$$

where the sum is over the free parameters in the problem. Ignoring terms of order $\delta\vec{x}^2$ and setting $\vec{F}(\vec{x}+\delta\vec{x})=\vec{0}$ gives us an expression for the corrections $\delta\vec{x}$ to $\vec{x}$:

$$\delta\vec{x} = -\left(J^TJ\right)^{-1}J^T\vec{F}, \tag{17}$$

$$J_{ij}\equiv\frac{\partial F_i}{\partial x_j}. \tag{18}$$

We then iterate until the corrections are smaller than some convenient cutoff value. In practice we stop the iteration process if either of the following conditions is true:

$$\sum_j|\delta x_j| < \delta x_{min}=0.0001 \text{ or } \sum_i|F_i| < F_{min}=0.0001. \tag{19}$$

In order to prevent the iteration process from spiraling off toward a nonsensical solution, we added the following additional requirement:

$$\text{if } \sqrt{\sum_i \delta x_i^2} > \delta x_{MAX}, \text{ then } \delta x_j \rightarrow \delta x_j \frac{\delta x_{MAX}}{\sqrt{\sum_i \delta x_i^2}}, \tag{20}$$

with $\delta x_{MAX} = 0.1$. For completeness the relevant partial derivatives are (after dropping the leading minus sign in equation 14)

$$\frac{\partial F_i}{\partial q_c} = -\frac{V(t_i)}{q_c}, \tag{21}$$

$$\frac{\partial F_i}{\partial t_{min}} = -\frac{q_c R_F}{\tau^2}\left[\frac{\tau}{t_i - t_{min} + t_0} - e^{-(t_i - t_{min} + t_0)/\tau}\left[Ei\left(\frac{t_i - t_{min} + t_0}{\tau}\right) - Ei\left(\frac{t_0}{\tau}\right)\right]\right], \tag{22}$$

for $t > t_{min}$.

Figure 2 shows a sample flash-ADC distribution from one of the strips with the curve for $V(t)$ deduced from the Newton-Raphson iteration procedure superimposed. Here the time-constant τ was fixed to 20 ns. The shape (at least for this event) is surprisingly well-described by my relatively simple model for the pulse shape.

We used a run with the anode voltage set to 1.75 kV to study the timing algorithms. The signals from each of the anode wires were discriminated by a Lecroy 2313 leading edge discriminator in CAMAC with a threshold set to 20 mV common to all channels. The resulting logic pulses were digitized by an F1 TDC module. The postamp gains for the wires was set to the minimum because raising the gains causes clipping of the pulses. Unless otherwise specified, the FADC timing was derived from the strip that had the largest amount of charge in the event. Figure 3 demonstrates that the correlation between the avalanche time as measured at the anode wires and one of the cathode planes is very good, as expected. We then measured the spread in the difference between these two methods for measuring the time of the signal on a wire. We fixed the number of anode wires firing per event to one. The top row of Figure 4 shows the distribution of t_{min} values from the simple method and the spread in time difference between these times and the time derived from the F1 TDC data. The Gaussian resolution of the difference distribution is 5.127 ± 0.081 ns. If we use the 2.75 ns value quoted above that we expect for this crude time method, this implies that the jitter in the F1 signal is about $\sigma_{F1} = 4.33$ ns. The bottom row shows the distributions for the Newton-Raphson timing method with τ set to 20 ns for all FADC channels. The resolution is 4.469 ± 0.063 ns – a noticeable improvement that corresponds to $\sigma_{FADC} \approx 1$ ns using $\sigma_{F1} = 4.33$ ns. This is a preliminary result that is hampered by jitter in the reference time from the F1 TDC/CAMAC discriminator combination. Inspection of the drift time

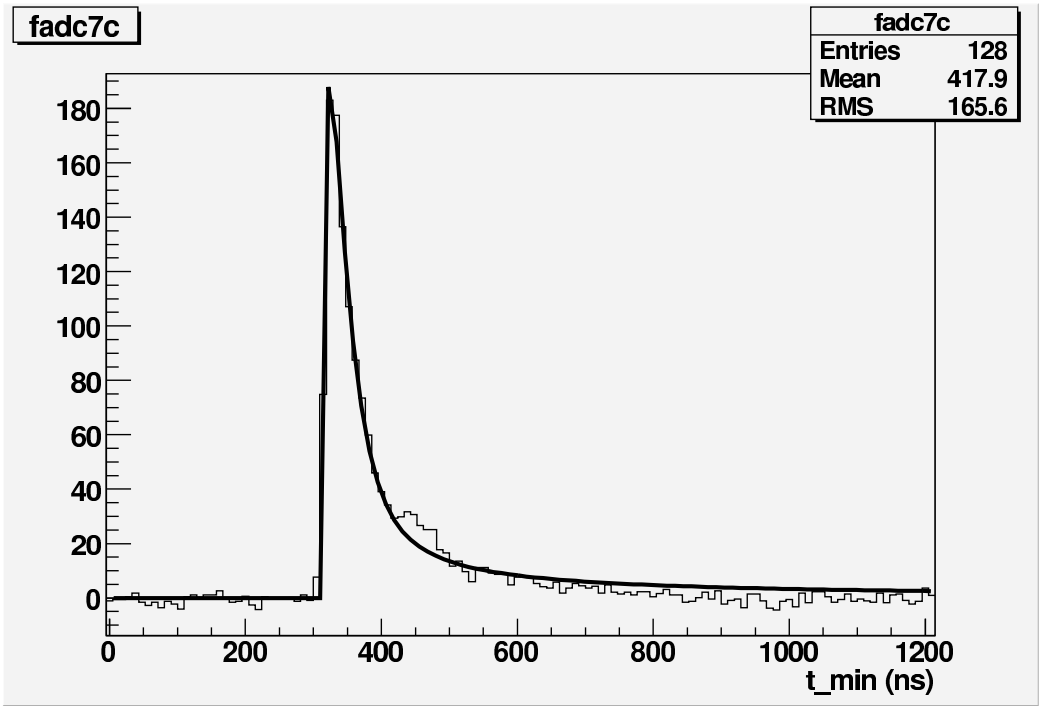

Figure 2: Sample pulse on one of the strips with the pulse-shape model result superimposed.

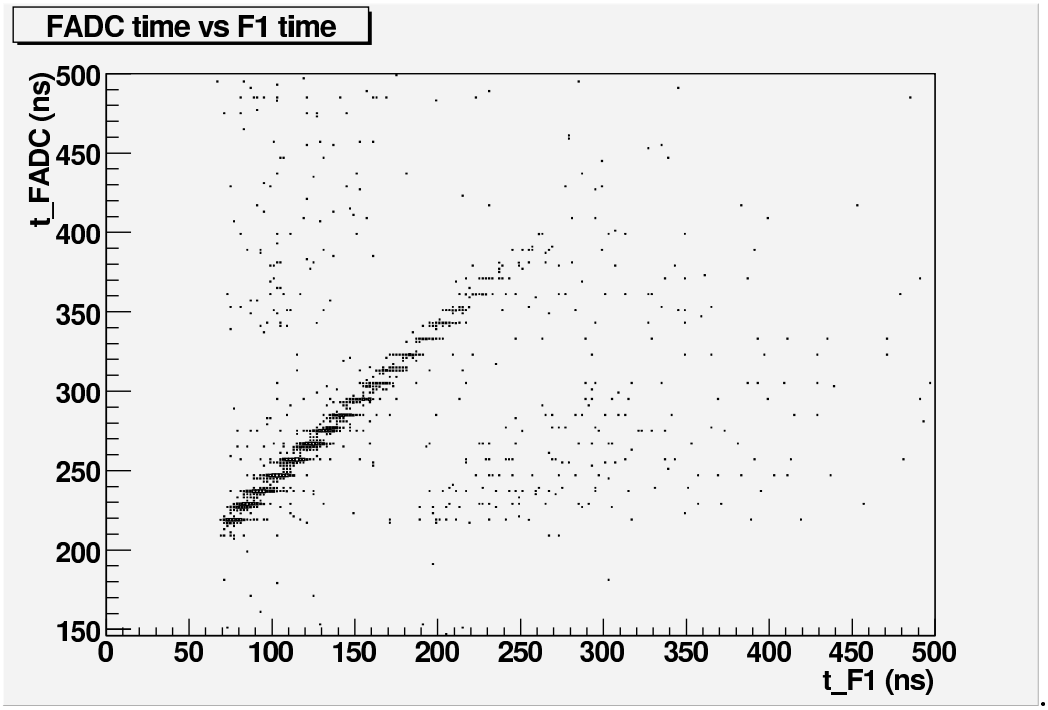

Figure 3: Correlation between time obtained from the anode wire and time obtained from the strip with the most charge in each event.

distribution reveals that this method does not really get rid of the picket-fence structure but merely softens the sharpness of the spikes.

The time constant τ is not likely to be same for every channel. We used the digitized signals from a pulser calibration run to estimate the variation in the time constants. We approximated the signal from the pulser as a difference in exponentials (for $t > 0$):

$$i(t) = \frac{q}{\tau_1 - \tau_2}\left(e^{-t/\tau_1} - e^{-t/\tau_2}\right), \tag{23}$$

for which the resulting time-dependent voltage measured with the flash-ADC (again assuming a single pole in the response function of the electronics) is

$$V(t) = -\frac{qR_F}{\tau_1 - \tau_2}\left(\frac{\tau_1}{\tau_1 - \tau}\left(e^{-t/\tau_1} - e^{-t/\tau}\right) - \frac{\tau_2}{\tau_2 - \tau}\left(e^{-t/\tau_2} - e^{-t/\tau}\right)\right). \tag{24}$$

Figure 5 shows a sample fit of one of the pulses from the calibration run. Generally, the time constants τ_1 and τ_2 for the model of the input pulse were small compared to the time constant τ for the model of the electronics response (*i.e.* $\tau_1, \tau_2 \ll \tau$). Figure 6 shows the distribution of values for τ for each of the seven FADC channels connected to strips (channel 0 was not used in the pulser run). Table 1 enumerates the mean values for τ (parameter p3 in the fit). Since the signals from the avalanche data seem to be wider than the pulser signals, we scaled the results in the second column such that the average was 20 ns. The resulting values were used in the Newton-Raphson procedure. This had no effect on the resolution; the revised value for $\sigma_{\Delta t}$ was 4.467 ± 0.061 ns. There seems to be very little sensitivity to the actual value for τ. Figure 7 shows the dependence of the timing resolution on the number of samples in the leading edge used in the calculation. Apart from the poor resolution when using the minimum number of samples needed to obtain values for the two parameters q_c and t_{min} there is no dependence on the number of samples.

3 Finding centroids

Previous studies[3] have indicated that the shape of the cathode charge distribution is well-described by a function of the form

$$\rho(\lambda) = \frac{q_c(\lambda)}{q_a} = K_1\left(1 - \tanh^2(K_2\lambda)\right), \tag{25}$$

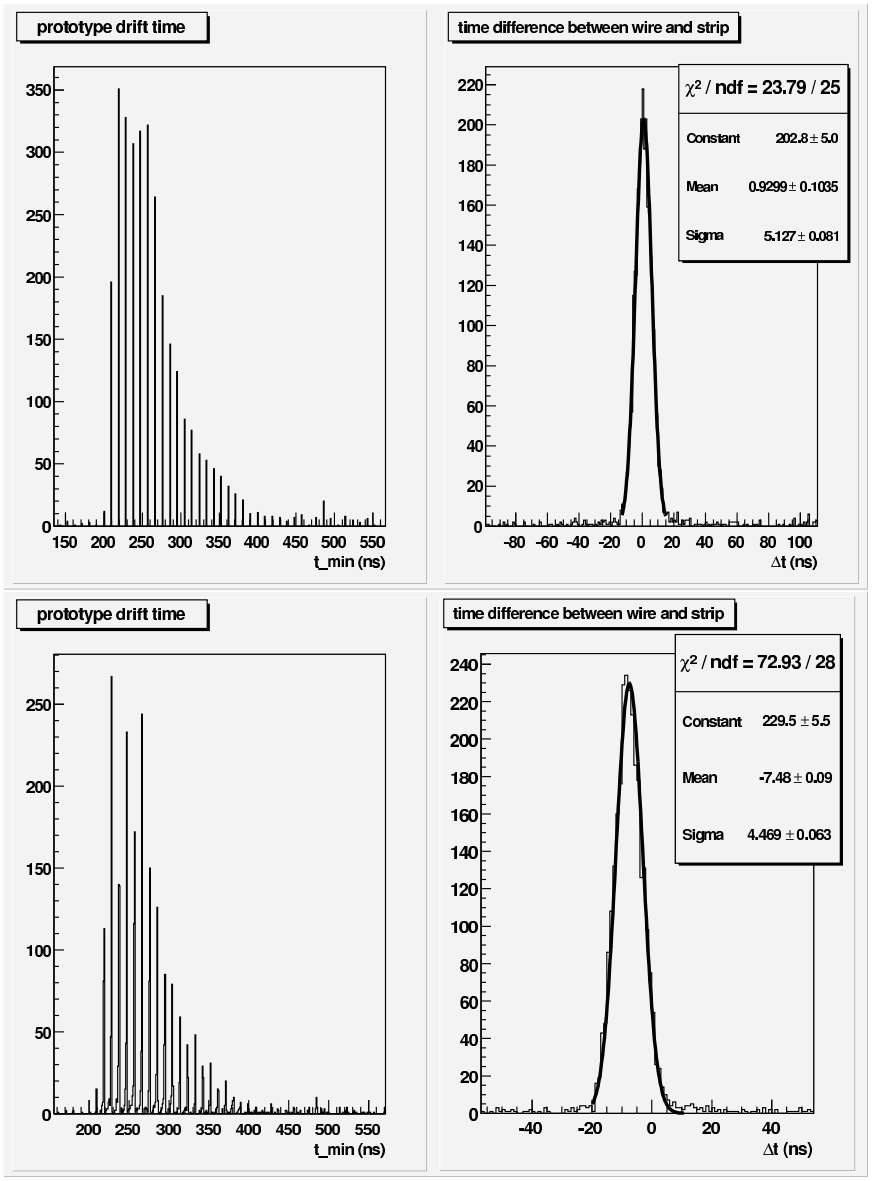

Figure 4: Comparison of the drift time distribution and FADC-F1 time difference for the simple leading edge method (top row) and the Newton-Raphson method (bottom row) with $\tau = 20$ ns.

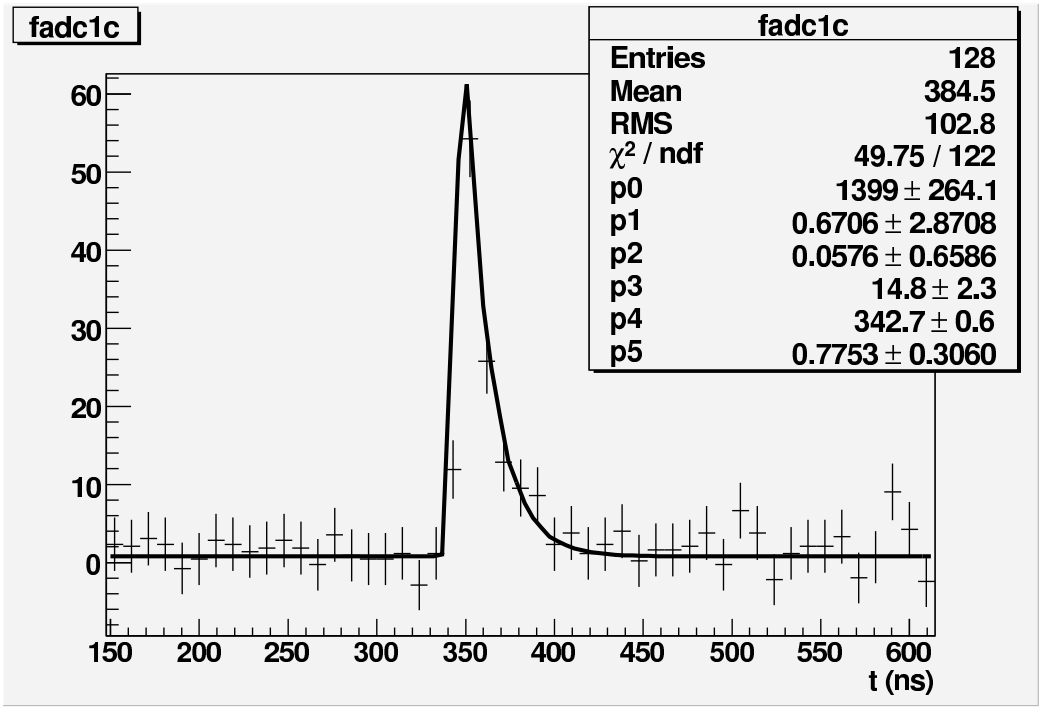

Figure 5: Sample fit of a pulse from a pulser calibration run.

Channel	τ (ns)	Scaled τ (ns)
1	15.99	20.19
2	18.77	23.70
3	15.38	19.42
4	14.59	18.42
5	17.28	21.82
6	13.83	17.46
7	15.04	18.99

Table 1: Mean values for τ for the preamp/postamp response function and the same values scaled so that the average is 20 ns.

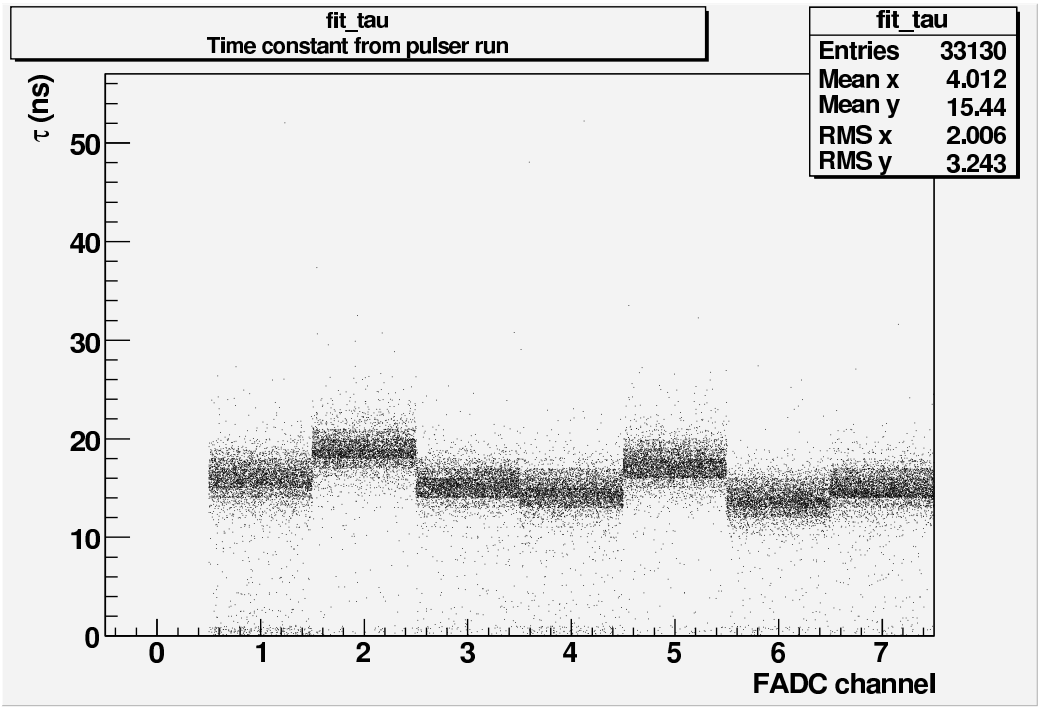

Figure 6: Distribution of time constant (τ) values from the pulser data.

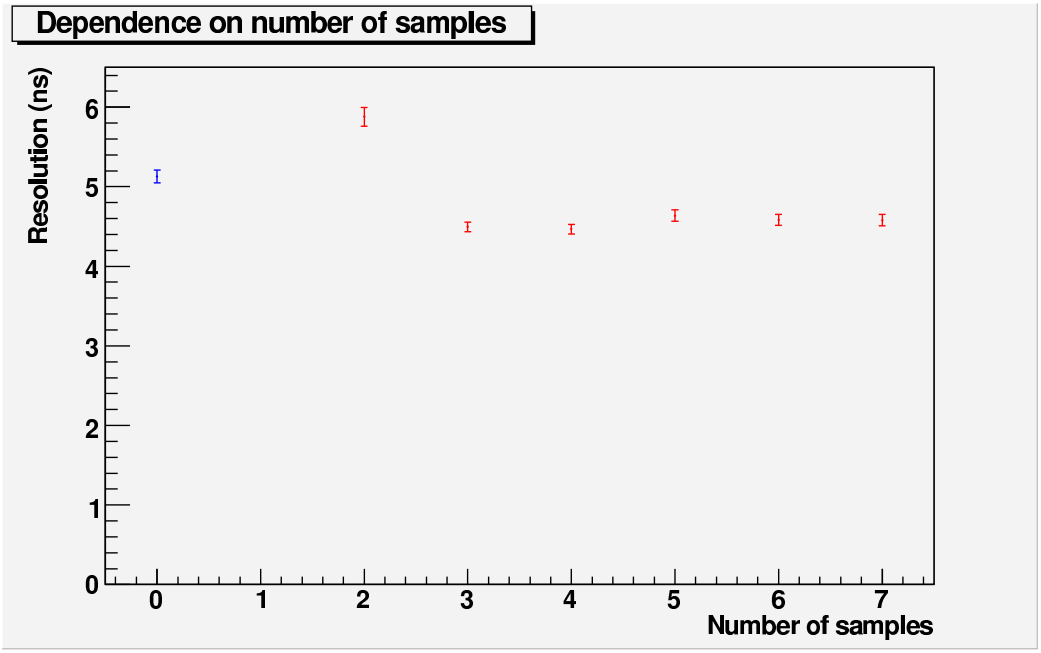

Figure 7: Dependence of time resolution on number of samples used in the iteration procedure. For comparison the resolution obtained from the simple method is shown at (number of samples) = 0.

where $\lambda = x/h$ with x being the coordinate transverse to the strips and h being the anode-to-cathode separation. K_1 and K_2 are empirical constants. To obtain the charge induced on a strip we need to integrate this distribution over the width of the strip. For a strip with width $2a$ centered at $\lambda' = x'/h$,

$$\frac{q_c(\lambda')}{q_a} = \frac{K_1}{K_2}\left[\tanh\left(K_2\left(\lambda' + \frac{a}{h}\right)\right) - \tanh\left(K_2\left(\lambda' - \frac{a}{h}\right)\right)\right]. \quad (26)$$

Requiring $\int_{-\infty}^{+\infty}\rho(\lambda)d\lambda = \frac{1}{2}$ determines $K_1 = K_2/4$. In our case the strips are at positions x_n quantized in steps of 5 mm. Assuming that the charge distribution is peaked at x_p, we define $\lambda_n = (x_p - x_n)/h$. For each distribution of charge over the strips in given plane there are three unknown quantities, namely q_a, x_p, and K_2. If we have measured the charge Q_n on three adjacent strips centered on the strip with the maximum charge, we have a non-linear system of equations (with $n = 1..3$):

$$F_n = Q_n - \frac{q_a}{4}\left[\tanh\left(K_2\left(\frac{x_p - x_n + a}{h}\right)\right) - \tanh\left(K_2\left(\frac{x_p - x_n - a}{h}\right)\right)\right] = 0. \quad (27)$$

This system of equations can be solved iteratively using the standard Newton-Raphson method, which is the same as the procedure described above with the simplification that because J is a square matrix,

$$\delta\vec{x} = -J^{-1}\vec{F}. \quad (28)$$

For completeness the relevant partial derivatives are:

$$\frac{\partial F_i}{\partial q_a} = -\frac{1}{4}\left[\tanh\left(K_2\left(\frac{x_p - x_i + a}{h}\right)\right) - \tanh\left(K_2\left(\frac{x_p - x_i - a}{h}\right)\right)\right], \quad (29)$$

$$\frac{\partial F_i}{\partial K_2} = -\frac{q_a}{4}\left[\left(\frac{x_p - x_i + a}{h}\right)\operatorname{sech}^2\left(K_2\left(\frac{x_p - x_i + a}{h}\right)\right) - \left(\frac{x_p - x_i - a}{h}\right)\operatorname{sech}^2\left(K_2\left(\frac{x_p - x_i - a}{h}\right)\right)\right], \quad (30)$$

$$\frac{\partial F_i}{\partial x_p} = -\frac{q_a K_2}{4h}\left[\operatorname{sech}^2\left(K_2\left(\frac{x_p - x_i + a}{h}\right)\right) - \operatorname{sech}^2\left(K_2\left(\frac{x_p - x_i - a}{h}\right)\right)\right]. \quad (31)$$

Previously, we obtained the best position resolution by fitting the charge distributions on the strips with equation 25 over five strips. The more strips we use to determine the centroid, the more noise we add. The further the strips are from the centroid, the less useful they are. Therefore we might

Wire position (mm)	Mathieson fit $\sigma_x(\mu\text{m})$ 5 strips	3 strips	Newton-Raphson $\sigma_x(\mu\text{m})$
270.6	182.0	165.5	181.0
280.6	195.1	203.7	187.9
290.6	191.8	195.8	180.8
300.6	176.0	180.1	166.3
310.6	202.6	187.7	179.8
330.5	196.3	202.1	191.7
340.5	210.4	215.5	200.7
350.5	195.6	198.8	172.6
Average:	193.7	193.8	182.6

Table 2: Comparison of position resolutions obtained from the Mathieson fitting method to the results of the Newton-Raphson iteration procedure. For this comparison the conventional charge-integrating ADCs were used.

expect to get better results with 3 strips using the Newton-Raphson method than with 5 strips using the old fitting method. This expectation is borne out by the data. Table 2 compares the resolutions for the reconstructed wire positions for the two different techniques for obtaining the centroids on the cathode planes. For this comparison we used the run with anode wires at 1750 V and read out both cathode views with the CAEN ADCs. We also required that only one wire fired in an event. The Newton-Raphson method gives slightly narrower peaks on average.

We will not be using the conventional charge-integrating ADCs in the final setup. It is important to demonstrate that we can obtain the same results using the Flash-ADCs. Figure 8 shows the reconstructed wire positions for the case where we use the Flash-ADC for one view and the conventional CAEN ADCs for the other view. Table 3 enumerates the Gaussian widths (σ) of the peaks. We find that the average resolution is about 12% larger than for the case where we used CAEN ADCs for both views. The cause of this discrepancy is still under investigation.

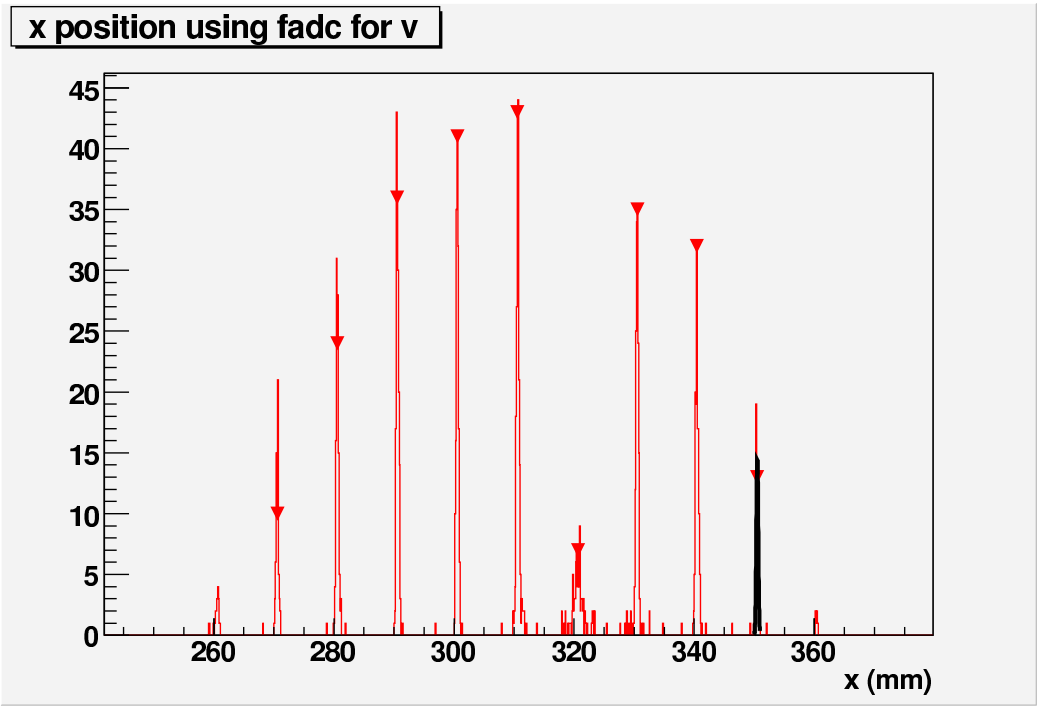

Figure 8: Wire positions reconstructed using Flash-ADC data for the v-view.

x (mm)	σ_x (μm)
270.6	218.5
280.6	200.9
290.6	195.9
300.6	191.2
310.6	209.0
330.5	207.6
340.5	247.4
350.5	158.8
Average:	203.7

Table 3: Resolution of wire positions reconstructed using Flash-ADC data for v-view.

References

[1] W.H. Press, S.A. Teukolsky, W.T. Vetterling, and B.P. Flannery, Numerical Recipes in C: The Art of Scientific Computing, 2nd edition (Cambridge, U.K.: Cambridge University Press, 1992), p. 134.

[2] ibid., pp. 379-383.

[3] S. Taylor and D.S. Carman, GlueX-doc-526-v1.